Int. J. Solids Structures Vol. 16, pp. 19–40
Pergamon Press Ltd., 1980. Printed in Great Britain

STRESS ANALYSIS FOR AN ELASTIC HALF SPACE CONTAINING AN EMBEDDED RIGID BLOCK

G. K. HARITOS† and L. M. KEER
Department of Civil Engineering, Northwestern University, Evanston, IL 60201, U.S.A.

(*Received* 22 *June* 1978; *in revised form* 11 *January* 1979)

Abstract—The plane elasticity problem of a finite, rigid rectangular block partially embedded in, and perfectly bonded to an elastic half space is investigated. The problem is formulated by the superposition of the solutions to the problems of horizontal and vertical line inclusions beneath an elastic half space. Substitution of these results into the boundary conditions appropriate for the embedded block problem leads to a system of coupled singular integral equations, whose unknowns are the normal and shear stress discontinuities between the bonded surfaces.

Two distinct sets of loads are applied to the embedded block, so that it either translates without rotation in the y-direction, or rotates about an axis in the z-direction.

Several important physical quantities are computed, e.g. the diffusion of the load from the block into the elastic half space for vertical translation and the rotational stiffness.

1. INTRODUCTION

This paper is concerned with the stress analysis of an elastic half space, in which a perfectly bonded, rigid rectangular block is partially embedded. The bond thickness is assumed to be sufficiently thin so that the displacements of the bonded surfaces are continuous. Within this context the problem is one of plane strain and can be considered appropriate to calculations that involve the stress distributions around foundations where the out-of-plane dimensions are very large when compared with the length or width of the rectangle. Alternatively, the problem can be viewed as one of generalized plane stress analyzing the load diffusion from a finite, rigid rectangular insert, partially embedded within a semi-infinite sheet, where the axis of the insert is perpendicular to the edge of the sheet. The geometry and coordinate system for such a block is shown in Fig. 1, where μ is the shear modulus and κ is related to Poisson's ratio by $\kappa = 3-4\nu$ (plane strain) or $\kappa = (3-\nu)/(1+\nu)$ (plane stress), and ν is Poisson's ratio.

Problems such as the one considered here have had a long history, which is best summarized in a paper by Muki and Sternberg[1], who consider the diffusion of load from a transverse tension bar into a semi-infinite elastic sheet. They reconsider the problem initially posed by Reissner[2], who considered the load transfer from a transverse stringer, a finite segment of which overlaps with, and is continuously bonded to, a semi-infinite elastic sheet. Theirs is essentially a contact problem in which the finite stringer is attached to the semi-infinite sheet and their objective is to obtain a systematic reduction of the problem to a Fredholm integral equation via two contact models, i.e. line-contact or area-contact.

The present analysis differs from theirs in that the sheet is assumed to be cut so that it has a finite rectangular notch at its surface. A perfectly matching rigid, rectangular insert is then bonded within this notch.

Loading is applied to this embedded insert so that it either translates without rotation in the vertical or horizontal direction, or rotates about an axis in the z-direction due to an applied moment. The plane strain case corresponds to an infinite, rectangular block embedded within an elastic half space undergoing vertical or horizontal translation, or rotation.

It should be noted that Muki and Sternberg have also dealt with the three-dimensional problem of load diffusion from an axially loaded rod to a half-space[3, 4]. In [3] the problem of the axial force decay in an infinite cylindrical elastic bar bonded to an infinite medium is dealt with. An approximate solution scheme for cross-sections of arbitrary shape is developed and

†Present address: Department of Civil Engineering, Engineering Mechanics and Materials, U.S. Air Force Academy, CO 80840, U.S.A.

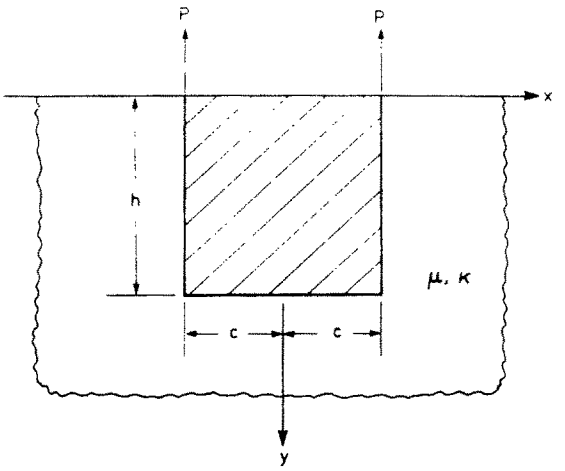

Fig. 1. Geometry and coordinate system for a partially embedded finite rigid block undergoing vertical translation.

compared to the exact one for the case of a circular bar. This scheme is then used in [4] to solve the problem of load diffusion from a bar of arbitrary uniform cross section partially embedded in, and bonded to a semi-infinite solid.

The solution of the considered problem is developed in successive stages. In Section 2 Green's functions are written for a horizontal and vertical line load beneath an elastic half space. This formulation allows the boundary value problem to be given as having boundary conditions only on the surface of the notch [5]. The results were derived using integral transform techniques, but they can also be derived by other methods. The primary references used for these derivations were the text by Sneddon [6], and the tables edited by Erdélyi [7].

Section 3 deals with the vertical translation of the finite rigid rectangular block partially embedded in, and perfectly bonded to an elastic half space, under an applied load $2P$ acting in the negative y-direction. The appropriate boundary conditions are written by superposing the horizontal and vertical inclusion results. The boundary conditions become the data for a system of singular integral equations, which can be solved numerically. It is noted that there are four points on the block that are singular: the intersection of the block with the free surface, $(\pm c, 0)$, and the lower corners of the block, $(\pm c, h)$. These singularities can be accounted for in the analysis by the establishment of appropriate relationships through an asymptotic expansion of the governing singular integral equations in the vicinity of these corners. It should be noted here that the solution of the transcendental equation derived for the corners $(\pm c, h)$ leads to two negative roots. Therefore, they both lead to singular contributions. The singular stress field is dominated by the largest singularity, and this is the one used in the present analysis. To the authors' knowledge, the only work that considers both negative roots at a corner such as the one encountered here, is a paper by Westmann [8], which deals with a wedge bonded to a half plane along a finite length. The solution for that problem was developed using Mellin transforms, and numerical results were obtained by use of a modified finite difference method. However, accounting for both negative roots is beyond the scope of this paper. A possibly simpler estimate for the numerical results is obtained by considering the analogous problem of two rigid vertical inclusions of length equal to the sides of the rigid block, and separated by a distance equal to the base of the block, partially embedded in and bonded to an elastic half-space, and each loaded by P in the negative y-direction. This problem is considered in [9]; a discussion of the results obtained is included in Section 5 of the present paper.

The case of horizontal displacement of the rigid block loaded by $2Q$, acting in the negative x-direction, and a moment M is also formulated in Section 3. The results obtained from the solution of this problem are given in [9], and they will not be reported in the present paper.

Section 4 investigates the rotation of the rigid block about an axis in the z-direction under the action of a moment M.

In Section 5 the method for obtaining numerical results is discussed. The collocation scheme introduced by Erdogan, Gupta and Cook [10] is used to solve the system of singular integral

equations governing each of the problems formulated in Sections 3 and 4. The method of solution allows the calculation of certain important physical quantities such as the diffusion of load from the block into the elastic half space for vertical translation and the rotational stiffness.

2. FORMULATION AND BASIC EQUATIONS

(a) *Horizontal inclusion in a half space*

The equations to be obtained here are for a bonded, rigid inclusion of length $2c$ located a depth h beneath the free surface, $y = 0$, of an elastic half space. The inclusion is assumed to have zero thickness and its geometry and coordinate system are shown in Fig. 2. If the discontinuities in the normal and shear stresses are designated by $A(x)$ and $B(x)$, respectively, then the following conditions must be satisfied:

$$\left.\begin{aligned} \tau_{yy}^{(2)} - \tau_{yy}^{(1)} &= A(x) \\ \tau_{xy}^{(2)} - \tau_{xy}^{(1)} &= B(x) \end{aligned}\right\} \quad y = h, \ -c \le x \le c. \tag{2.1}$$

In addition to the above equations, the following continuity and boundary conditions must be satisfied:

$$\left.\begin{aligned} u_x^{(2)} - u_x^{(1)} &= 0 \\ u_y^{(2)} - u_y^{(1)} &= 0 \end{aligned}\right\} \quad y = h, \ -c \le x \le c \tag{2.2}$$

$$\tau_{yy}(x,0) = \tau_{xy}(x,0) = 0, \quad 0 \le |x| < \infty \tag{2.3}$$

where the superscripts (1), (2) define the regions above and below the inclusion.

In terms of the stress discontinuities, $A(x)$ and $B(x)$ defined above, the displacement derivatives and stresses throughout the half space are given as

$$\frac{\partial u_x^I}{\partial x}(x,y) = \frac{1}{4\pi(\kappa+1)\mu}\left\{\int_{-c}^{c} A(s)K_{N1}(x,y;s)\,ds + \int_{-c}^{c} B(s)K_{S1}(x,y;s)\,ds\right\} \tag{2.4}$$

$$\frac{\partial u_y^I}{\partial x}(x,y) = \frac{1}{4\pi(\kappa+1)\mu}\left\{\int_{-c}^{c} A(s)K_{N2}(x,y;s)\,ds + \int_{-c}^{c} B(s)K_{S2}(x,y;s)\,ds\right\} \tag{2.5}$$

$$\frac{\partial u_x^I}{\partial y}(x,y) = \frac{1}{4\pi(\kappa+1)\mu}\left\{\int_{-c}^{c} A(s)K_{N3}(x,y;s)\,ds + \int_{-c}^{c} B(s)K_{S3}(x,y;s)\,ds\right\} \tag{2.6}$$

$$\frac{\partial u_y^I}{\partial y}(x,y) = \frac{1}{4\pi(\kappa+1)\mu}\left\{\int_{-c}^{c} A(s)K_{N4}(x,y;s)\,ds + \int_{-c}^{c} B(s)K_{S4}(x,y;s)\,ds\right\} \tag{2.7}$$

$$\tau_{xx}^I(x,y) = \frac{1}{2\pi(\kappa+1)}\left\{\int_{-c}^{c} A(s)K_{N5}(x,y;s)\,ds + \int_{-c}^{c} B(s)K_{S5}(x,y;s)\,ds\right\} \tag{2.8}$$

$$\tau_{yy}^I(x,y) = \frac{1}{2\pi(\kappa+1)}\left\{\int_{-c}^{c} A(s)K_{N6}(x,y;s)\,ds + \int_{-c}^{c} B(s)K_{S6}(x,y;s)\,ds\right\} \tag{2.9}$$

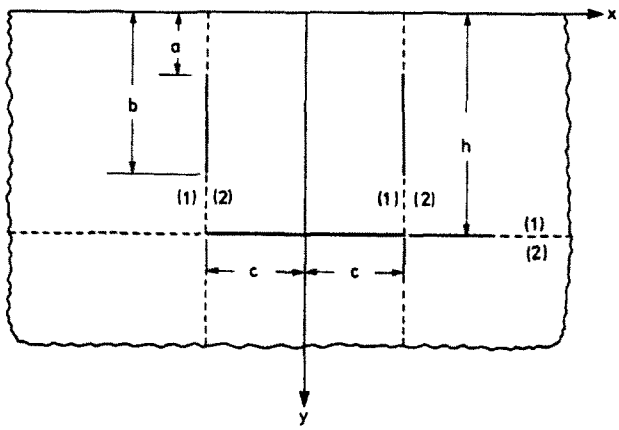

Fig. 2. Superposition solution.

$$\tau^{I}_{xy}(x,y)=\frac{1}{2\pi(\kappa+1)}\left\{\int_{-c}^{c}A(s)K_{N7}(x,y;s)\,ds+\int_{-c}^{c}B(s)K_{S7}(x,y;s)\,ds\right\} \tag{2.10}$$

The functions K_{Ni} and K_{Si}, $i=1,2,\ldots,7$, are given in the Appendix and they are rational functions of x and y with both numerators and denominators being polynomials in x and y.

Equations (2.4)–(2.10) were derived using integral transform techniques [6, 7], but they can also be derived by other methods.

(b) *Vertical inclusion in a half space*

Here, the case of a vertical inclusion of length $(b-a)$ perpendicular to the free surface of an elastic half space, $y=0$, is solved (Fig. 2). Let the jumps in the normal and shear stresses across the inclusion be $C(y)$ and $D(y)$, respectively; then, the following relationships must hold:

$$\left.\begin{aligned}\tau^{(2)}_{xx}-\tau^{(1)}_{xx}&=C(y)\\ \tau^{(2)}_{xy}-\tau^{(1)}_{xy}&=D(y)\end{aligned}\right\}\quad x=c,\ a\le y\le b; \tag{2.11}$$

$$\left.\begin{aligned}u^{(2)}_{x}-u^{(1)}_{x}&=0\\ u^{(2)}_{y}-u^{(1)}_{y}&=0\end{aligned}\right\}\quad x=c,\ a\le y\le b; \tag{2.12}$$

$$\tau_{yy}(x,0)=\tau_{xy}(x,0)=0,\quad y=0,\quad 0\le|x|<\infty. \tag{2.13}$$

For this case the superscripts (1), (2) refer to the regions to the left and right of the inclusion, respectively.

In terms of the stress jumps, $C(y)$ and $D(y)$, defined by eqns (2.11), the displacement derivatives and stresses within the half space are given as

$$\frac{\partial u^{II}_{x}}{\partial x}(x,y)=\frac{1}{4\pi(\kappa+1)\mu}\left\{\int_{a}^{b}C(t)L_{N1}(x,y;t)dt+\int_{a}^{b}D(t)L_{S1}(x,y;t)dt\right\} \tag{2.14}$$

$$\frac{\partial u^{II}_{y}}{\partial x}(x,y)=\frac{1}{4\pi(\kappa+1)\mu}\left\{\int_{a}^{b}C(t)L_{N2}(x,y;t)dt+\int_{a}^{b}D(t)L_{S2}(x,y;t)dt\right\} \tag{2.15}$$

$$\frac{\partial u^{II}_{x}}{\partial y}(x,y)=\frac{1}{4\pi(\kappa+1)\mu}\left\{\int_{a}^{b}C(t)L_{N3}(x,y;t)dt+\int_{a}^{b}D(t)L_{S3}(x,y;t)dt\right\} \tag{2.16}$$

$$\frac{\partial u^{II}_{y}}{\partial y}(x,y)=\frac{1}{4\pi(\kappa+1)\mu}\left\{\int_{a}^{b}C(t)L_{N4}(x,y;t)dt+\int_{a}^{b}D(t)L_{S4}(x,y;t)dt\right\} \tag{2.17}$$

$$\tau^{II}_{xx}(x,y)=\frac{1}{2\pi(\kappa+1)}\left\{\int_{a}^{b}C(t)L_{N5}(x,y;t)dt+\int_{a}^{b}D(t)L_{S5}(x,y;t)dt\right\} \tag{2.18}$$

$$\tau^{II}_{yy}(x,y)=\frac{1}{2\pi(\kappa+1)}\left\{\int_{a}^{b}C(t)L_{N6}(x,y;t)dt+\int_{a}^{b}D(t)L_{S6}(x,y;t)dt\right\} \tag{2.19}$$

$$\tau^{II}_{xy}(x,y)=\frac{1}{2\pi(\kappa+1)}\left\{\int_{a}^{b}C(t)L_{N7}(x,y;t)dt+\int_{a}^{b}D(t)L_{S7}(x,y;t)dt\right\} \tag{2.20}$$

where the functions L_{Ni} and L_{Si}, $i=1,2,\ldots,7$, are given in the Appendix. It is noted that the superscript II is used to identify displacement derivatives and stresses associated with the vertical inclusion at $x=c$, while I was used in connection with the horizontal inclusion located at $y=h$. To obtain the equations associated with a vertical inclusion of length $(b-a)$, located at $x=-c$, one replaces c by $-c$ in eqns (A15)–(A28), $C(t)$ by $E(t)$, and $D(t)$ by $F(t)$ in eqns (2.14)–(2.20). For this case the superscript III will be used. These equations will not be listed here but will be incorporated in the following sections.

3. VERTICAL DISPLACEMENT OF EMBEDDED BLOCK

The results of the preceding section are now superposed to formulate the problem of a rigid block perfectly bonded to an elastic half space and loaded as shown in Fig. 1. The limits of integration for the vertical inclusions (solutions II and III) are taken as $a=0$ and $b=h$ (Fig. 2).

The boundary conditions for this problem are given next:

$$\left.\begin{aligned}\frac{\partial u_x}{\partial x}&=\frac{\partial u_x^{\mathrm{I}}}{\partial x}(x,h)+\frac{\partial u_x^{\mathrm{II}}}{\partial x}(x,h)+\frac{\partial u_x^{\mathrm{III}}}{\partial x}(x,h)=0\\ \frac{\partial u_y}{\partial x}&=\frac{\partial u_y^{\mathrm{I}}}{\partial x}(x,h)+\frac{\partial u_y^{\mathrm{II}}}{\partial x}(x,h)+\frac{\partial u_y^{\mathrm{III}}}{\partial x}(x,h)=0\end{aligned}\right\},\quad -c\le x\le c,\ y=h; \tag{3.1}$$

$$\left.\begin{aligned}\frac{\partial u_x}{\partial y}&=\frac{\partial u_x^{\mathrm{I}}}{\partial y}(-c,y)+\frac{\partial u_x^{\mathrm{II}}}{\partial y}(-c,y)+\frac{\partial u_x^{\mathrm{III}}}{\partial y}(-c,y)=0\\ \frac{\partial u_y}{\partial y}&=\frac{\partial u_y^{\mathrm{I}}}{\partial y}(-c,y)+\frac{\partial u_y^{\mathrm{II}}}{\partial y}(-c,y)+\frac{\partial u_y^{\mathrm{III}}}{\partial y}(-c,y)=0\end{aligned}\right\},\quad 0\le y\le h,\ x=-c; \tag{3.2}$$

$$\left.\begin{aligned}\frac{\partial u_x}{\partial y}&=\frac{\partial u_x^{\mathrm{I}}}{\partial y}(c,y)+\frac{\partial u_x^{\mathrm{II}}}{\partial y}(c,y)+\frac{\partial u_x^{\mathrm{III}}}{\partial y}(c,y)=0\\ \frac{\partial u_y}{\partial y}&=\frac{\partial u_y^{\mathrm{I}}}{\partial y}(c,y)+\frac{\partial u_y^{\mathrm{II}}}{\partial y}(c,y)+\frac{\partial u_y^{\mathrm{III}}}{\partial y}(c,y)=0\end{aligned}\right\},\quad 0\le y\le h,\ x=c. \tag{3.3}$$

Equations (3.1)–(3.3) represent a system of six singular integral equations, which are given next:

$$\int_{-c}^{c}A(s)K_{N1}(x,h;s)\mathrm{d}s+\int_{-c}^{c}B(s)K_{S1}(x,h;s)\mathrm{d}s+\int_0^h C(t)L_{N1}(x,h;t)\mathrm{d}t+\int_0^h D(t)L_{S1}(x,h;t)\mathrm{d}t$$
$$+\int_0^h E(t)\bar{L}_{N1}(x,h;t)\mathrm{d}t+\int_0^h F(t)\bar{L}_{S1}(x,h;t)\mathrm{d}t=0,\quad -c\le x\le c; \tag{3.4}$$

$$\int_{-c}^{c}A(s)K_{N2}(x,h;s)\mathrm{d}s+\int_{-c}^{c}B(s)K_{S2}(x,h;s)\mathrm{d}s+\int_0^h C(t)L_{N2}(x,h;t)\mathrm{d}t+\int_0^h D(t)L_{S2}(x,h;t)\mathrm{d}t$$
$$+\int_0^h E(t)\bar{L}_{N2}(x,h;t)\mathrm{d}t+\int_0^h F(t)\bar{L}_{S2}(x,h;t)\mathrm{d}t=0,\quad -c\le x\le c; \tag{3.5}$$

$$\int_{-c}^{c}A(s)K_{N3}(-c,y;s)\mathrm{d}s+\int_{-c}^{c}B(s)K_{S3}(-c,y;s)\mathrm{d}s+\int_0^h C(t)L_{N3}(-c,y;t)\mathrm{d}t$$
$$+\int_0^h D(t)L_{S3}(-c,y;t)\mathrm{d}t+\int_0^h E(t)\bar{L}_{N3}(-c,y;t)\mathrm{d}t=0,\quad 0\le y\le h; \tag{3.6}$$

$$\int_{-c}^{c}A(s)K_{N4}(-c,y;s)\mathrm{d}s+\int_{-c}^{c}B(s)K_{S4}(-c,y;s)\mathrm{d}s+\int_0^h C(t)L_{N4}(-c,y;t)\mathrm{d}t$$
$$+\int_0^h D(t)L_{S4}(-c,y;t)\mathrm{d}t+\int_0^h F(t)\bar{L}_{S4}(-c,y;t)\mathrm{d}t=0,\quad 0\le y\le h; \tag{3.7}$$

$$\int_{-c}^{c}A(s)K_{N3}(c,y;s)\mathrm{d}s+\int_{-c}^{c}B(s)K_{S3}(c,y;s)\mathrm{d}s+\int_0^h C(t)L_{N3}(c,y;t)\mathrm{d}t+\int_0^h E(t)\bar{L}_{N3}(c,y;t)\mathrm{d}t$$
$$+\int_0^h F(t)\bar{L}_{S3}(c,y;t)\mathrm{d}t=0,\quad 0\le y\le h; \tag{3.8}$$

$$\int_{-c}^{c}A(s)K_{N4}(c,y;s)\mathrm{d}s+\int_{-c}^{c}B(s)K_{S4}(c,y;s)\mathrm{d}s+\int_0^h D(t)L_{S4}(c,y;t)\mathrm{d}t+\int_0^h E(t)\bar{L}_{N4}(c,y;t)\mathrm{d}t$$
$$+\int_0^h F(t)\bar{L}_{S4}(c,y;t)\mathrm{d}t=0,\quad 0\le y\le h. \tag{3.9}$$

The barred kernels $\bar{L}_{Ni}$ and $\bar{L}_{Si}$, $i=1,2,\ldots,4$, are readily obtained from the corresponding unbarred kernels given in the Appendix by replacing c by $-c$. It is also noted that the boundary conditions for the integral equations are homogeneous. However, the input data will be given in the form of subsidiary conditions that involve the load $2P$ applied to the block and the constraints, when the symmetry appropriate to the considered problem is used.

Since eqns (3.4)–(3.9) deal with the geometry of corners, their limit near the corners must

produce definite relationships in the neighborhood of such corners. These relationships may be directly obtained from the governing singular integral equations, after the contributing parts are isolated from the entire equations. First, the order of the singularity at the intersection of the free surface with a vertical inclusion will be established by considering the appropriate contributory terms. Adjusting the coordinate system to account for the right-hand inclusion, the terms leading to the determination of the singularity at the free surface are given as

$$\int_0^h C(t)\left[\frac{2\kappa}{y-t}+\frac{\kappa^2+1}{y+t}+\frac{4t(y-t)}{(y+t)^3}\right]\mathrm{d}t=0, \tag{3.10}$$

where y is approaching zero. A second equation, identical to (3.10), is obtained for $D(t)$. Assuming solutions of the form,

$$C(t)=\bar{C}(t)t^{\eta-1}, \tag{3.11}$$

$$D(t)=\bar{D}(t)t^{\eta-1}, \tag{3.12}$$

where $0<\eta<1$, the following eigenvalue equation is deduced for the determination of η:

$$\sin^2\left(\frac{\pi\eta}{2}\right)=\frac{(\kappa+1)^2}{4\kappa}-\frac{1}{\kappa}\eta^2. \tag{3.13}$$

Except for a minor change in notation, eqn (3.13) is identical to that determined by Williams [11] for a right-angle corner of an elastic plate in extension with fixed-free boundary conditions. When eqn (3.13) is solved for $\nu=0.3$ (plane strain), the result is

$$\eta=0.71117. \tag{3.14}$$

Conditions at the corners (c, h) and $(-c, h)$ can be established in a similar manner through the use of eqns (3.4)–(3.9), where the following asymptotic forms are assumed for the sought functions:

$$A(s)=\bar{A}(s)(c^2-s^2)^{\zeta-1},\quad B(s)=\bar{B}(s)(c^2-s^2)^{\zeta-1};$$
$$C(t)=\bar{C}(t)^{\eta-1}(h-t)^{\eta-1},\ldots,F(t)=\bar{F}(t)t^{\eta-1}(h-t)^{\zeta-1} \tag{3.15}$$

where $0<\zeta<1$. The relationships which must be satisfied in the vicinity of the corner (c, h) are found to be

$$\kappa\cos(\pi\zeta)B_0+(\kappa-\zeta)\cos\left(\frac{\pi\zeta}{2}\right)C_0+\zeta\sin\left(\frac{\pi\zeta}{2}\right)D_0=0 \tag{3.16a}$$

$$\kappa\cos(\pi\zeta)A_0+\zeta\sin\left(\frac{\pi\zeta}{2}\right)C_0+(\kappa+\zeta)\cos\left(\frac{\pi\zeta}{2}\right)D_0=0 \tag{3.16b}$$

$$\zeta\sin\left(\frac{\pi\zeta}{2}\right)A_0+(\kappa+\zeta)\cos\left(\frac{\pi\zeta}{2}\right)B_0+\kappa\cos(\pi\zeta)C_0=0 \tag{3.16c}$$

$$(\kappa-\zeta)\cos\left(\frac{\pi\zeta}{2}\right)A_0+\zeta\sin\left(\frac{\pi\zeta}{2}\right)B_0+\kappa\cos(\pi\zeta)D_0=0, \tag{3.16d}$$

and for $(-c, h)$

$$\kappa\cos(\pi\zeta)B_0'+(\kappa-\zeta)\cos\left(\frac{\pi\zeta}{2}\right)E_0-\zeta\sin\left(\frac{\pi\zeta}{2}\right)F_0=0 \tag{3.17a}$$

$$\kappa\cos(\pi\zeta)A_0'-\zeta\sin\left(\frac{\pi\zeta}{2}\right)E_0+(\kappa+\zeta)\cos\left(\frac{\pi\zeta}{2}\right)F_0=0 \tag{3.17b}$$

$$(\kappa-\zeta)\cos(\pi\zeta)A_0'-\zeta\sin\left(\frac{\pi\zeta}{2}\right)B_0'+\kappa\cos(\pi\zeta)F_0=0 \tag{3.17c}$$

$$-\zeta\sin\left(\frac{\pi\zeta}{2}\right)A_0'+(\kappa+\zeta)\cos\left(\frac{\pi\zeta}{2}\right)B_0'+\kappa\cos(\pi\zeta)E_0=0. \tag{3.17d}$$

In eqns (3.16) and (3.17) the following notation is used:

$$A_0 = \bar{A}(c)(2c)^{\zeta-1}/h^{\eta-1}, \quad B_0 = \bar{B}(c)(2c)^{\zeta-1}/h^{\eta-1},$$
$$A_0' = \bar{A}(-c)(2c)^{\zeta-1}/h^{\eta-1}, \quad B_0' = \bar{B}(-c)(2c)^{\zeta-1}/h^{\eta-1},$$
$$C_0, D_0, E_0, F_0 = \bar{C}(h), \bar{D}(h), \bar{E}(h), \bar{F}(h). \tag{3.18}$$

Equations (3.16) and (3.17) lead to the same eigenvalue equation, namely

$$\left[\kappa^2 \sin^2\left(\frac{3\pi\zeta}{2}\right) - \zeta^2\right]\left[\kappa^2 \sin^2\left(\frac{\pi\zeta}{2}\right) - \zeta^2\right] = 0, \tag{3.19}$$

where ζ is determined from

$$\sin\left(\frac{3\pi\zeta}{2}\right) = \pm\frac{1}{\kappa}\zeta, \tag{3.20}$$

which is in agreement with Williams' result for a fixed–fixed $3\pi/2$-corner of an elastic plate in extension[11]. If the positive sign in eqn (3.20) is chosen and $\nu = 0.3$ (plane strain), the result is

$$\zeta = 0.59516. \tag{3.21}$$

It should be noted that eqn (3.20) with the negative sign also yields a root in the interval of interest, $\zeta = 0.75904$; however, since the numerical scheme used to obtain numerical results[10] can only accommodate one of these roots, the gravest one, given by eqn (3.21) will be used.

Equations (3.4)–(3.9) represent a system of six singular integral equations, which along with appropriate subsidiary conditions can be solved for the six unknown stress discontinuities $A(s)$, $B(s), \ldots, F(t)$. However, by taking advantage of the symmetric nature of the problem, the number of unknowns can be reduced to *four*, since the following relationships must hold:

$$E(y) = -C(y), \quad F(y) = D(y). \tag{3.22}$$

Thus, the subsidiary conditions associated with eqns (3.4)–(3.9) are not needed and will not be listed here. Equation (3.22) is incorporated to write eqns (3.4), (3.5), (3.8) and (3.9) in the following form:

$$\int_{-c}^{c} A(s)K_{N1}(x,h;s)\mathrm{d}s + \int_{-c}^{c} B(s)K_{S1}(x,h;s)\mathrm{d}s + \int_0^h C(t)[L_{N1}(x,h;t) - \bar{L}_{N1}(x,h;t)]\mathrm{d}t$$
$$+ \int_0^h D(t)[L_{S1}(x,h;t) + \bar{L}_{S1}(x,h;t)]\mathrm{d}t = 0, \quad -c \le x \le c; \tag{3.23}$$

$$\int_{-c}^{c} A(s)K_{N2}(x,h;s)\mathrm{d}s + \int_{-c}^{c} B(s)K_{S2}(x,h;s)\mathrm{d}s + \int_0^h C(t)[L_{N2}(x,h;t) - \bar{L}_{N2}(x,h;t)]\mathrm{d}t$$
$$+ \int_0^h D(t)[L_{S2}(x,h;t) + \bar{L}_{S2}(x,h;t)]\mathrm{d}t = 0, \quad -c \le x \le c; \tag{3.24}$$

$$\int_{-c}^{c} A(s)K_{N3}(c,y;s)\mathrm{d}s + \int_{-c}^{c} B(s)K_{S3}(c,y;s)\mathrm{d}s + \int_0^h C(t)[L_{N3}(c,y;t) - \bar{L}_{N3}(c,y;t)\mathrm{d}t$$
$$+ \int_0^h D(t)\bar{L}_{S3}(c,y;t)\mathrm{d}t = 0, \quad 0 \le y \le h; \tag{3.25}$$

$$\int_{-c}^{c} A(s)K_{N4}(c,y;s)\mathrm{d}s + \int_{-c}^{c} B(s)K_{S4}(c,y;s)\mathrm{d}s + \int_0^h C(t)[-\bar{L}_{N4}(c,y;t)]\mathrm{d}t$$
$$+ \int_0^h D(t)[L_{S4}(c,y;t) + \bar{L}_{S4}(c,y;t)]\mathrm{d}t = 0, \quad 0 \le y \le h. \tag{3.26}$$

Note that eqns (3.6) and (3.7) are eliminated as unnecessary. It is also clear that $A(x)$ must be

symmetric and $B(x)$ antisymmetric in the range $-c \leq x \leq c$. These properties will be incorporated in the numerical analysis.

Since the unknown stress discontinuities, $A(s)$, $B(s)$, $C(t)$ and $D(t)$, have integrable singularities at the end points, in addition to eqns (3.23)–(3.26), they must also satisfy the following subsidiary conditions[10]:

$$\int_{-c}^{c} A(x)\mathrm{d}x + 2\int_{0}^{h} D(y)\mathrm{d}y = 2P; \tag{3.27}$$

$$\int_{0}^{c} \left[\frac{\partial u_x}{\partial x}\right]_{y=0} \mathrm{d}x = 0; \tag{3.28}$$

$$\int_{0}^{c} \left[\frac{\partial u_y}{\partial x}\right]_{y=0} \mathrm{d}x - \int_{0}^{h} \left[\frac{\partial u_y}{\partial y}\right]_{x=0} \mathrm{d}y = 0; \tag{3.29}$$

$$\int_{-c}^{c} B(x)\,\mathrm{d}x = 0. \tag{3.30}$$

The choice of eqns (3.27)–(3.30) as the subsidiary conditions appropriate for this problem warrants a brief discussion. It was found that extreme care must be exercised in selecting the correct combination of conditions from several available relationships which could, conceivably, serve as subsidiary conditions. The task is to prescribe conditions which supplement the boundary conditions in describing the problem, without using redundant ones, and, of course, without violating any of the conditions that apply to mixed boundary value problems. Including redundant conditions has the same effect as using the same equation twice (i.e. renders the matrix of coefficients singular), while the subtle manner in which certain factors enter the problem creates such dangers as overconstraining the problem by prescribing tractions and displacements along the same direction.

The governing singular integral equations (eqns 3.23–3.26) ensure that the base and the sides of the block do not rotate and do not elongate (shrink). Equation (3.27) represents the global equilibrium for the rigid block in the vertical direction. Equation (3.30) is a statement requiring $B(x)$ to be antisymmetric. This, along with eqn (3.22) which requires that $E(y) = -C(y)$, satisfies the equation of equilibrium in the horizontal direction. Equations (3.28) and (3.29) impose kinematic restrictions on the problem. Equation (3.28) fixes the sides of the block at $x = \pm c$, while eqn (3.29) requires that the base and the sides of the block do not move relative to each other in the vertical direction.

Equations (3.23)–(3.30) are therefore the relationships appropriate for the solution of the problem of a rigid block embedded in an elastic half space and undergoing vertical displacement.

The problem of a rigid block embedded in an elastic half space and forced to translate in the negative x-direction without rotation, under the action of a horizontal load $2Q$, and a moment M, as shown in Fig. 3, is also formulated here.

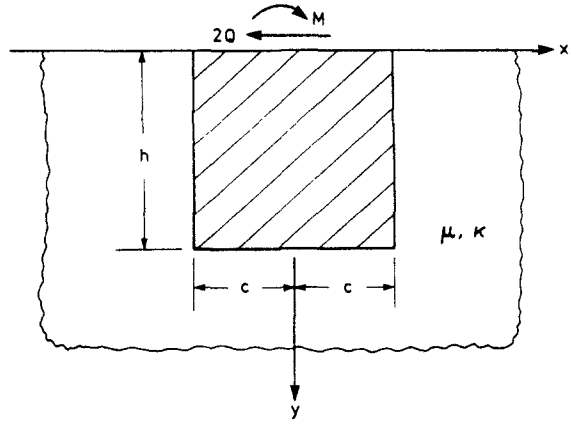

Fig. 3. Geometry and coordinate system for an embedded block undergoing horizontal translation or rotation.

The boundary conditions appropriate for this problem are the same as those given in eqns (3.1)–(3.3) for the vertical translation problem. The symmetry and the subsidiary conditions appropriate for the horizontal translation case are given next:

$$E(y) = C(y), \quad F(y) = -D(y); \tag{3.31}$$

$$A(x) = -A(-x), \quad B(x) = B(-x); \tag{3.32}$$

$$\int_{-c}^{c} B(x)\,dx + 2\int_{0}^{h} C(y)\,dy = 2Q; \tag{3.33}$$

$$\int_{0}^{c} \left[\frac{\partial u_y}{\partial x}\right]_{y=0} dx = 0; \tag{3.34}$$

$$\int_{0}^{c} \left[\frac{\partial u_x}{\partial x}\right]_{y=0} dx - \int_{0}^{h} \left[\frac{\partial u_x}{\partial y}\right]_{x=0} dy = 0; \tag{3.35}$$

$$\int_{0}^{c} A(x)\,dx = 0. \tag{3.36}$$

The horizontal displacement of the rigid block problem is similar to the vertical displacement problem; therefore, numerical results for this problem are not presented in this paper. However, the numerical analysis was performed and the results are reported in [9].

4. ROTATION OF EMBEDDED BLOCK

This section investigates the problem of a partially embedded rigid block that rotates through an angle α under the action of a moment M, as shown in Fig. 3. Here, the tangential load Q is set equal to zero. The boundary conditions for this problem are given next:

$$\frac{\partial u_x}{\partial x} = 0, \quad \frac{\partial u_y}{\partial x} = \alpha; \quad -c \le x \le c, \; y = h; \tag{4.1}$$

$$\frac{\partial u_x}{\partial y} = -\alpha, \quad \frac{\partial u_y}{\partial y} = 0; \quad 0 \le y \le h, \; x = \pm c. \tag{4.2}$$

Substitution of the horizontal and vertical inclusion results derived in Section 2 in eqns (4.1) and (4.2) leads to a system of six governing singular integral equations with generalized Cauchy kernels. However, the symmetric nature of the problem allows for the elimination of two of the unknown stress discontinuities, since the relationships given next must be satisfied:

$$E(y) = C(y); \quad F(y) = -D(y). \tag{4.3}$$

Therefore, only four of the equations represented by eqns (4.1) and (4.2) are necessary for the solution to this problem. Note that the symmetry of the problem also requires that $A(x)$ is antisymmetric, and $B(x)$ symmetric in the range $-c \le x \le c$.

Equation (4.3) is incorporated to write the equations represented by eqn (4.1) and those of (4.2) at $x = c$ in the following form.

$$\frac{1}{4\pi(\kappa+1)\mu}\left\{\int_{-c}^{c} A(s)K_{N1}(x,h;s)ds + \int_{-c}^{c} B(s)K_{S1}(x,h;s)ds + \int_{0}^{h} C(t)[L_{N1}(x,h;t) + \bar{L}_{N1}(x,h;t)dt + \int_{0}^{h} D(t)[L_{S1}(x,h;t) - \bar{L}_{S1}(x,h;t)]dt = 0, \quad -c \le x \le c; \tag{4.4}$$

$$\frac{1}{4\pi(\kappa+1)\mu}\left\{\int_{-c}^{c} A(s)K_{N2}(x,h;s)ds + \int_{-c}^{c} B(s)K_{S2}(x,h;s)ds + \int_{0}^{h} C(t)[L_{N2}(x,h;t) + \bar{L}_{N2}(x,h;t)]dt + \int_{0}^{h} D(t)[L_{S2}(x,h;t) - \bar{L}_{S2}(x,h;t)]dt\right\} = \alpha, \quad -c \le x \le c; \tag{4.5}$$

$$\frac{1}{4\pi(\kappa+1)\mu}\left\{\int_{-c}^{c} A(s)K_{N3}(c,y;s)\mathrm{d}s + \int_{-c}^{c} B(s)K_{S3}(c,y;s)\mathrm{d}s + \int_{0}^{h} C(t)[L_{N3}(c,y;t) + \bar{L}_{N3}(c,y;t)]\mathrm{d}t + \int_{0}^{h} D(t)[-\bar{L}_{S3}(c,y;t)]\mathrm{d}t\right\} = -\alpha, \quad 0 \le y \le h; \tag{4.6}$$

$$\frac{1}{4\pi(\kappa+1)\mu}\left\{\int_{-c}^{c} A(s)K_{N4}(c,y;s)\mathrm{d}s + \int_{-c}^{c} B(s)K_{S4}(c,y;s) + \int_{0}^{h} C(t)\bar{L}_{N4}(c,y;t)\mathrm{d}t + \int_{0}^{h} D(t)[L_{S4}(c,y;t) - \bar{L}_{S4}(c,y;t)]\mathrm{d}t\right\} = 0, \quad 0 \le y \le h. \tag{4.7}$$

The kernels appearing in eqns (4.4)–(4.7) have been defined previously. Note that the relationships in the vicinity of the corner (c, h), given by eqns (3.16), are also applicable to this problem. The order of the singularities at the points $(\pm c, 0)$, and $(\pm c, h)$ was derived previously, and is given by eqns (3.14) and (3.21), respectively.

The unknown functions $A(s)$, $B(s)$, $C(t)$ and $D(t)$ have integrable singularities at the end points. Thus, eqns (4.4)–(4.7) must be supplemented by additional conditions, and the ones appropriate for this problem are given next:

$$\int_{-c}^{c} B(x)\mathrm{d}x + 2\int_{0}^{h} C(y)\mathrm{d}y = 0; \tag{4.8}$$

$$\int_{0}^{c} \left[\frac{\partial u_y}{\partial x}\right]_{y=0} \mathrm{d}x = c\alpha; \tag{4.9}$$

$$\int_{0}^{c} \left[\frac{\partial u_x}{\partial x}\right]_{y=0} \mathrm{d}x - \int_{0}^{h} \left[\frac{\partial u_x}{\partial y}\right]_{x=0} \mathrm{d}y = h\alpha; \tag{4.10}$$

$$\int_{-c}^{c} A(x)\mathrm{d}x = 0. \tag{4.11}$$

Equation (4.8) represents the global equilibrium equation for the rigid block in the x-direction. Equilibrium in the y-direction is satisfied by eqn (4.11), which requires that $A(x)$ is antisymmetric, in association with eqn (4.3), requiring that $F(y) = -D(y)$. Equations (4.9) and (4.10) impose kinematic restrictions on the problem. Equation (4.9) prescribes the translation of the corner $(c, 0)$ of the block in the y-direction, while eqn (4.10) gives the relationship between the horizontal displacements of points $(c, 0)$ and $(0, h)$ on the block. It should be noted that the usual small angle approximations have been employed in writing eqns (4.9), (4.10).

5. NUMERICAL ANALYSIS AND DISCUSSIONS

(a) *Numerical analysis*

The objective of the numerical analysis is to solve numerically the systems of governing singular integral equations with the corresponding subsidiary conditions, derived in the previous sections, for the unknown stress discontinuities.

The equations are normalized by introducing the following variable changes:

$$x = c\bar{x}, \quad s = c\bar{s}; \tag{5.1}$$

$$y = \frac{h}{2}(1+\bar{y}), \quad t = \frac{h}{2}(1+\bar{t}). \tag{5.2}$$

In addition, the stress discontinuities are given forms that reflect their correct singularities at the corners (and the surface). For the case of vertical displacement of the rigid block the following substitutions are made:

$$A(s) = \frac{P}{c}\bar{A}(\bar{s})(1-\bar{s}^2)^{\zeta-1}; \quad B(s) = \frac{P}{c}\bar{B}(\bar{s})(1-\bar{s}^2)^{\zeta-1}; \tag{5.3}$$

$$C(t)=\frac{2P}{h}\bar{C}(\bar{t})(1-\bar{t})^{\zeta-1}(1+\bar{t})^{\eta-1};$$

$$D(t)=\frac{2P}{h}\bar{D}(\bar{t})(1-\bar{t})^{\zeta-1}(1+\bar{t})^{\eta-1}. \tag{5.4}$$

To normalize the equations derived for the case of rotation of the rigid block (see Section 4) the following substitutions are needed:

$$A(s)=\frac{2\pi(\kappa+1)\mu ac}{\kappa}\bar{A}(\bar{s})(1-\bar{s}^2)^{\zeta-1};$$

$$B(s)=\frac{2\pi(\kappa+1)\mu ac}{\kappa}\bar{B}(\bar{s})(1-\bar{s}^2)^{\zeta-1}; \tag{5.5}$$

$$C(t)=\frac{2\pi(\kappa+1)\mu ah}{\kappa}\bar{C}(\bar{t})(1-\bar{t})^{\zeta-1}(1+\bar{t})^{\eta-1};$$

$$D(t)=\frac{2\pi(\kappa+1)\mu ah}{\kappa}\bar{D}(\bar{t})(1-\bar{t})^{\zeta-1}(1+\bar{t})^{\eta-1}. \tag{5.6}$$

The substitutions given in eqns (5.1) and (5.2) also apply to this problem.

Equations (5.1)–(5.6) will appropriately normalize the governing singular integral equations and the subsidiary conditions so that the numerical analysis may be conducted. An adjustment is required in eqn (5.1) for normalizing eqns (3.28), (3.29), (4.9) and (4.10); instead of $x = c\bar{x}$, take

$$x = c(1+\bar{x})/2. \tag{5.7}$$

For convenience, the parameter γ is introduced, and is defined as

$$\gamma = c/h. \tag{5.8}$$

It should be noted that for the case of rotation of the rigid block, it becomes necessary to assign a specific numerical value to either c or h. Thus, for that problem h is given unit length, and therefore γ becomes equal to c.

The numerical scheme to be used in this analysis is that described in Erdogan, Gupta and Cook[10], and is a collocation scheme based upon formulas for Gaussian integration (see Stroud and Secrest[12]). The integration points, $\bar{s}_i$, $\bar{t}_k$, and the collocation points, $\bar{x}_j$, $\bar{y}_l$, are defined as the roots of the Jacobi polynomials as follows:

$$P_N^{(\zeta-1,\zeta-1)}(\bar{s}_i)=0; \quad P_{N-1}^{(\zeta,\zeta)}(\bar{x}_j)=0; \tag{5.9}$$

$$P_N^{(\zeta-1,\eta-1)}(\bar{t}_k)=0; \quad P_{N-1}^{(\zeta,\eta)}(\bar{y}_l)=0. \tag{5.10}$$

The corresponding weights are obtained from the Gauss to Jacobi integration formula (see [12]).

Note that since the subsidiary conditions, which impose kinematic restrictions on all problems, require integrations to be performed along $y = 0$ and $x = 0$, additional integration points and weights are needed. The integration points appropriate to the interval $(0, c)$ along $y = 0$ are obtained from

$$P_N^{(\eta-1,0)}(\bar{x}_i)=0 \tag{5.11}$$

while the ones for $(0, h)$ along $x = 0$ are obtained from the Legendre polynomials, as the Gauss formula for numerical integration may be used in this case, since there are no singularities at the end points of the interval. The zeros of the Legendre polynomials (integration points), and the weights associated with the Gauss formula can be obtained from several sources (see, e.g. Abramowitz and Stegun[13]).

The asymptotic relationships in the vicinity of the corners $(\pm c, h)$ are in the forms given by eqns (3.16) and (3.17), where, for the case of vertical translation, the following relationships are valid:

$$A_0 = \bar{A}(1)/2^{\eta}\gamma^{\zeta}, \quad B_0 = \bar{B}(1)/2^{\eta}\gamma^{\zeta};$$
$$A_0' = \bar{A}(-1)/2^{\eta}\gamma^{\zeta}, \quad B_0' = \bar{B}(-1)/2^{\eta}\gamma^{\zeta}; \tag{5.12}$$

$$C_0, D_0, E_0, F_0 = \bar{C}(1), \bar{D}(1), \bar{E}(1), \bar{F}(1). \tag{5.13}$$

For the rotation of the rigid block problem eqn (5.12) is replaced by:

$$A_0 = 2^{1-\eta}\gamma^{2-\zeta}\bar{A}(1), \quad B_0 = 2^{1-\eta}\gamma^{2-\zeta}\bar{B}(1);$$
$$A_0' = 2^{1-\eta}\gamma^{2-\zeta}\bar{A}(-1), \quad B_0' = 2^{1-\eta}\gamma^{2-\zeta}\bar{B}(-1). \tag{5.14}$$

The barred quantities in eqns (5.12)–(5.14) have already been defined.

The procedure for obtaining solutions is the same for both types of loading applied to the rigid block, and is as follows. The symmetries of $A(s)$ and $B(s)$ are used to collapse the parts of the normalized equations containing them, thereby eliminating N of the unknown quantities. The problem is thus reduced to finding the solution to a system of $3N$ simultaneous algebraic equations in the $3N$ unknowns $\bar{A}(\bar{s}_i)$, $\bar{B}(\bar{s}_i)$, $\bar{C}(\bar{t}_k)$ and $\bar{D}(\bar{t}_k)$, where $i = 1, 2, \ldots, N/2$ and $k = 1, 2, \ldots, N$. The governing singular integral equations provide $3N$-4 equations, and the subsidiary conditions supply four more for a total of $3N$. By taking advantage of the antisymmetry of $B(x)$ (eqn 3.30) and of $A(x)$ (eqn 4.11), we can rewrite them as

$$B(0) = 0 \tag{3.30'}$$

$$A(0) = 0. \tag{4.11'}$$

The quantities $B(0)$, $A(0)$ are expressed as polynomials with $N/2$ terms by use of the Lagrange interpolation formula (see, e.g. Davis[14]).

(b) *Results and discussion*

The numerical analysis was completed for a range of the geometric parameter $\gamma(0.05 \leq \gamma \leq 8)$, and for Poisson's ratio (plane strain) of $\nu = 0.3$. The rate of convergence was tested by varying the number of points used at eight point intervals, from $N = 16$ to $N = 48$. The convergence of the global results appeared satisfactory and will be discussed in detail later. All results presented in this paper will be given for $N = 48$. The results for the respective problems of vertical displacement and rotation of an embedded rectangular block will be given next.

Vertical displacement. The load diffusion curves for several values of γ are shown in Fig. 4 for the case when the block moves vertically without rotation. The load acting on the block at a distance y below the surface is given as a fraction of the total load, where both load and distance have been put in dimensionless form. The load given by the intersection of the load-diffusion curves and the $y = h$ axis represents the load carried by the base of the block for each γ. Analogous to the block problem is that of two parallel inclusions, each subjected to a vertical load P and having no rotation. The results for this problem can be compared with those of the vertical displacement for the block. The load diffusion, calculated for the two-inclusion case, is shown in Fig. 5, where it is compared to the rigid block results; the solid lines represent values obtained from Fig. 4, and the dashed lines represent the two-inclusion case. These latter curves go to zero at $y = h$, since there is no base to carry part of the load. Furthermore, the dashed and solid curves are relatively close provided that $0 < y < 0.8\,h$. Thus, for relatively slender blocks, a solution which ignored the base would give approximately valid results. Figure 6 shows the percentage of the applied load P carried by the side of the rectangular block as a function of c/h. As expected, when c/h is small most of the load is carried by the sides; as c/h increases the base carries a larger share of the load. When γ is approximately equal to 0.42, the sides and the base each carry half the load.

Figures 7 and 8 show the variations, respectively, of the discontinuities in the normal

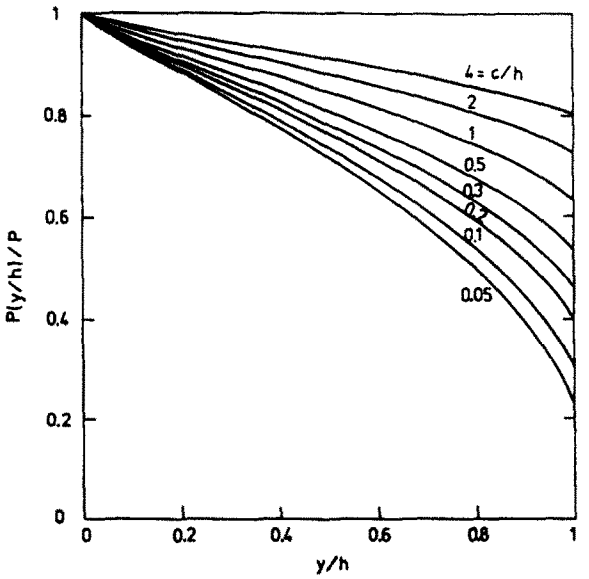

Fig. 4. Vertical Displacement: Load diffusion for various values of c/h.

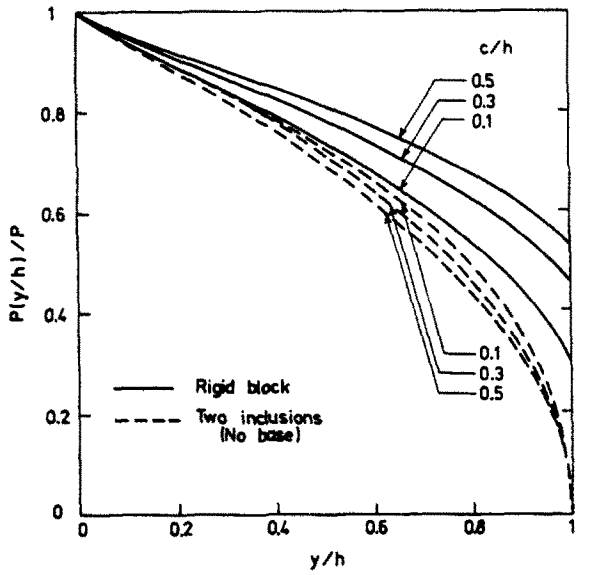

Fig. 5. Vertical Displacement: Comparison of load diffusion curves for the rigid block and the two-inclusion problems.

stresses along the base of the block, and those in the shear stresses along the sides for several values of c/h. Since a zero stress state prevails throughout the rigid block, these stress discontinuities represent the *actual* stress distributions along the walls of the elastic body surrounding the block, as is evident from the definitions of $A(x)$, $B(x)$, $C(y)$ and $D(y)$. Also, since the normal stresses are symmetric along the base, they are plotted only for $0 < x < c$ and exhibit singular behavior at the end $x = c$. The shear stresses are plotted for $0 < y < h$, and singular behavior is noted near both ends, $y = 0$, h. It is further observed that the magnitudes of both $A(x)$ and $D(y)$ vary proportionately with the amount of load carried by the base and the sides, respectively. Thus, the magnitude of $A(x)$ increases with γ, while the magnitude of $D(y)$ decreases as γ increases.

One estimate of the accuracy of the results may be obtained by calculating the displacements in the y-direction along the surface of the block $y = 0$, relative to the midpoint (0, 0). Since the block translates as a rigid body along y, these displacements should be small when compared to those obtained from the solution of the two-inclusion problem undergoing vertical displace-

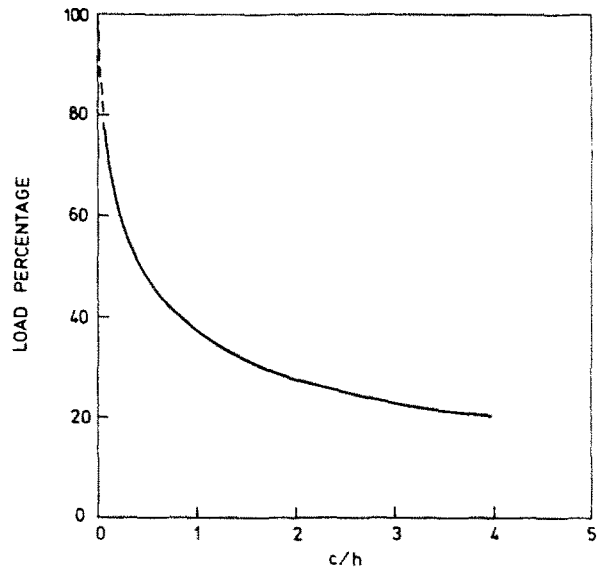

Fig. 6. Vertical Displacement: Percentage of the applied load P carried by each side of the rectangular block as a function of $\gamma = c/h$.

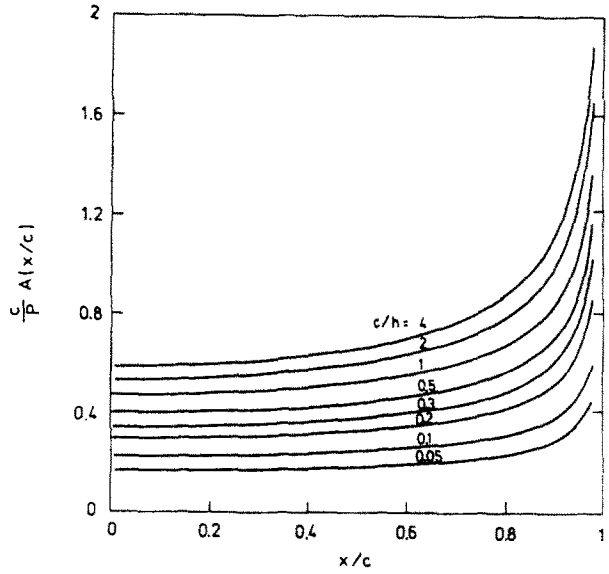

Fig. 7. Vertical Displacement: Normal stresses acting on base of block vs distance from center for several values of c/h.

ment. The results of this comparison are given in Table 1. It is noted that the displacements at the corner $x = c$ for the two inclusion problem vary from being approximately 18 times greater than the block displacements (for $\gamma = 0.3$), to being 175 times greater (for $\gamma = 4$). The displacements obtained for the rigid block problem tended to oscillate about zero, while the ones for the two inclusion problem grew with distance from (0, 0), as expected. It should be added that for $\gamma < 0.3$, the value of the ratio $|u_{y_1}/u_{y_2}|$ approaches unity. That is, as $\gamma = c/h$ becomes smaller, the presence (or absence) of the base has little or no effect on the results calculated near the surface. Therefore, a comparison of those results for the purposes of Table 1 would have little meaning, since the surface displacements are already small to within the accuracy of the solution.

Rotation. Results obtained for the problem of rotation of the embedded rigid block are presented in Figs. 9–13. The normal and shear stresses acting on the base of the block are given in Figs. 9 and 10 as functions of the distance from the midpoint, for several values of c/h. The normal and shear stress distributions along the sides of the block for $0 < y < h$, are plotted,

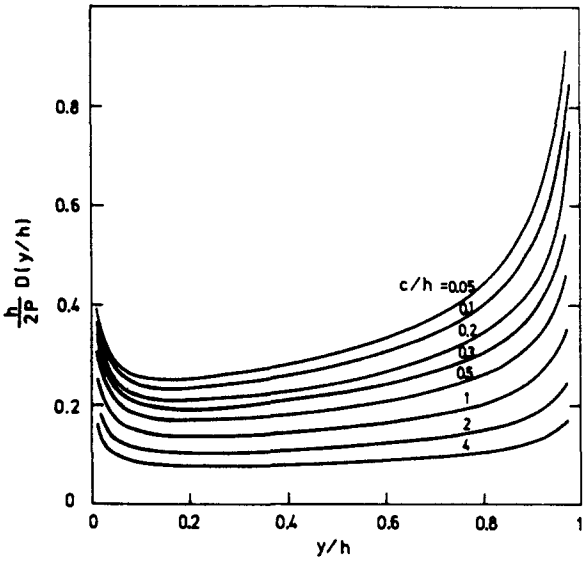

Fig. 8. Vertical Displacement: Shear stresses acting on side of block vs distance from free surface for various values of c/h.

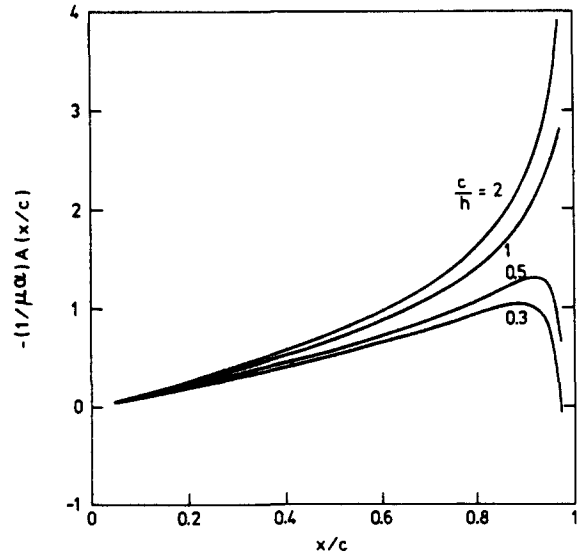

Fig. 9. Rotation: Normal stress distribution at $y = h$, $0 < x < c$, for various values of c/h.

Table 1. Vertical Displacement: Comparison of the y-displacements relative to the midpoint at the surface $y = 0$ of the rigid block (u_{y_b}) and the two-inclusion (u_{y_2}) problems for several values of $\gamma = c/h$

x/c \ c/h	$\lvert u_{y_b}/u_{y_2}\rvert$				
	0.3	0.5	1	2	4
0.2	0.3092	0.0547	0.0018	0.0028	0.0016
0.4	0.0154	0.0119	0.0101	0.0011	0.0010
0.6	0.2421	0.0461	0.0051	0.0002	0.0007
0.8	0.0258	0.0132	0.0092	0.0047	0.0015
1	0.0544	0.0178	0.0149	0.0081	0.0057

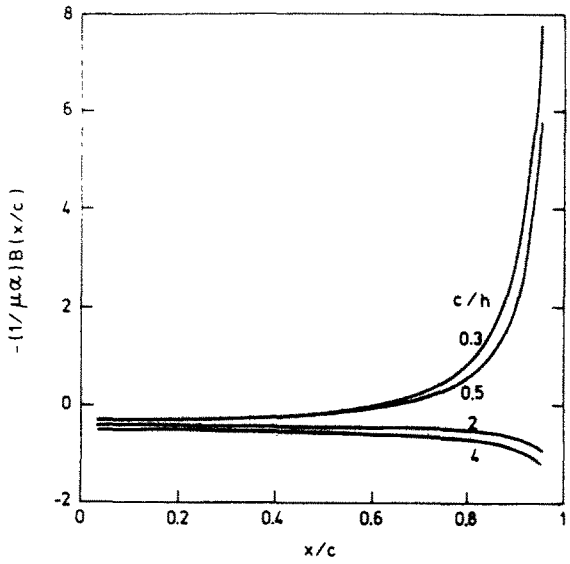

Fig. 10. Rotation: Shear stress distribution at $y = h$, $0 < x < c$, for various values of c/h.

respectively, in Figs. 11 and 12. The curves show the variation of the magnitude and sign of the stresses with γ. It should be noted that Figs. 9 and 10 indicate that the base stresses become bounded at the corner (c, h) for some value of $\gamma = c/h$. Therefore for this particular value of γ, the second root found ($\zeta - 1 = -0.24096$) may be the governing singularity in the vicinity of the corners $(\pm c, h)$.

A better understanding of the mechanics of the problem can be obtained by examining the moment equilibrium equation for the block, which is given next:

$$M = -\int_{-c}^{c} A(x)x\,dx + h\int_{-c}^{c} B(x)\,dx + 2\int_{0}^{h} C(y)y\,dy - 2c\int_{0}^{h} D(y)\,dy. \tag{5.15}$$

In writing eqn (5.15) use has been made of eqn (4.3). Using the symmetries of $A(x)$ and $B(x)$ appropriate for the rotation problem, and incorporating eqns (5.1), (5.2), (5.5) and (5.6), eqn (5.15) is rewritten in the normalized form given next:

$$\frac{1}{\mu h^2}\frac{M}{\alpha} = \frac{\pi(\kappa+1)}{\kappa}\Bigg[-4\gamma^3\int_0^1 \bar{A}(\bar{x})\bar{x}(1-\bar{x}^2)^{\zeta-1}\,d\bar{x} + 4\gamma^2\int_0^1 \bar{B}(\bar{x})(1-\bar{x}^2)^{\zeta-1}\,d\bar{x}$$
$$+\int_{-1}^{1} \bar{C}(\bar{y})(1+\bar{y})(1-\bar{y})^{\zeta-1}(1+\bar{y})^{\eta-1}\,d\bar{y} - 2\gamma\int_{-1}^{1} \bar{D}(\bar{y})(1-\bar{y})^{\zeta-1}(1+\bar{y})^{\eta-1}\,d\bar{y}\Bigg]. \tag{5.16}$$

Equation (5.16) may be written as

$$\frac{1}{\mu h^2}\frac{M}{\alpha} = A_S + B_S + C_S + D_S, \tag{5.17}$$

where the definitions of the quantities $A_S, \ldots, D_S$ are readily obtained by comparing eqns (5.16) and (5.17). The ratio $M/\mu h^2\alpha$ represents a measure of the rotational stiffness of the partially embedded rigid block. Therefore, the quantities A_S, B_S, C_S and D_S represent the contribution made to the stiffness by the stresses $A(x)$, $B(x)$, $C(y)$ and $D(y)$, respectively. Table 2 shows the variation of these quantities with γ. Note that the contribution of the normal stresses acting on the base of the block become significant only for $\gamma \geq 1$, while the opposite is true for the normal stresses acting on the sides (their contribution becomes more important as γ becomes smaller). It is also observed that the contribution of the base shear stresses to the total stiffness remains proportionately low for all values of γ, while that of the side shear stresses increases with γ.

By dividing $M/\mu h^2\alpha$ by γ^2, one obtains a new ratio, namely $M/\mu c^2\alpha$. These two ratios are

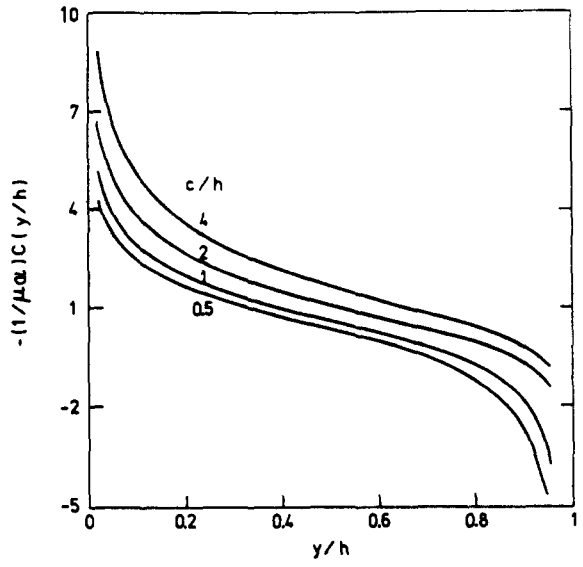

Fig. 11. Rotation: Normal stresses acting on the side of the block for $0 < y < h$, for several values of c/h.

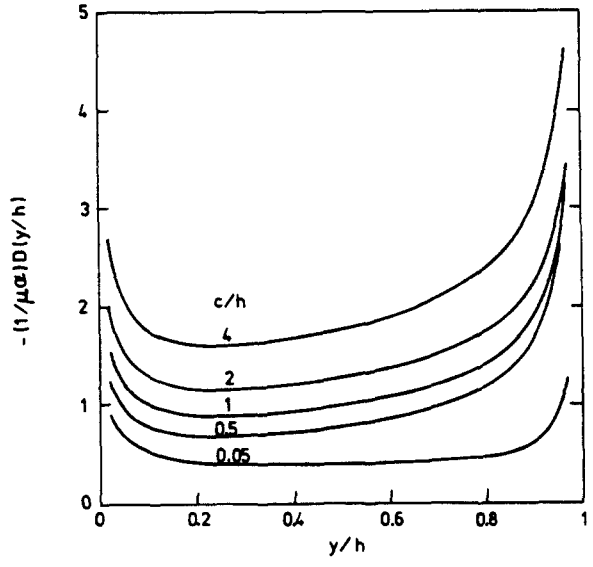

Fig. 12. Rotation: Shear stress distribution along the side of the block for $0 < y < h$, shown for several values of c/h.

Table 2. Rotation: Variation of the contributions of the stresses to the rotational stiffness of the embedded block with γ

c/h	A_S	B_S	C_S	D_S
0.05	−0.002	−0.236	1.232	−0.061
0.1	−0.006	−0.505	1.550	0.147
0.2	−0.020	−1.026	2.115	0.372
0.3	−0.036	−1.568	2.739	0.664
0.5	0.002	−2.091	3.350	1.356
1	1.123	−0.083	1.738	2.913
2	6.424	2.680	−0.255	6.656
4	27.685	4.369	−0.959	18.175

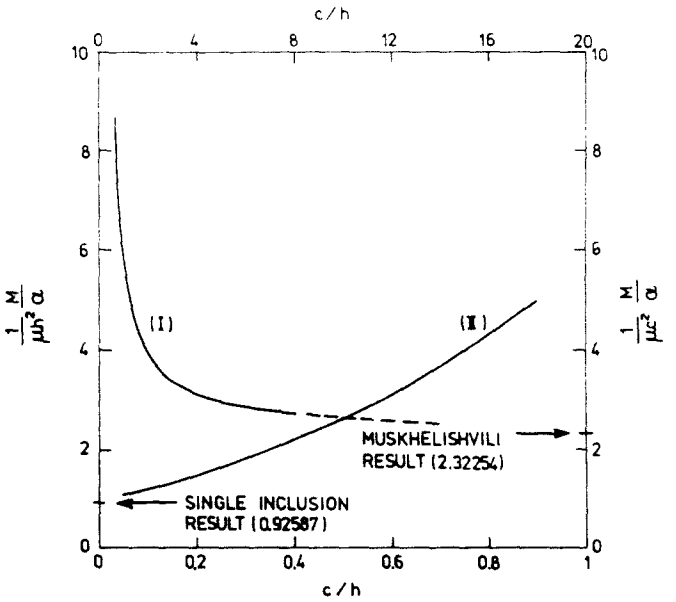

Fig. 13. Rotation: Stiffness for moment applied to rigid block (curve I: right ordinate, upper abscissa; curve II: left ordinate, lower abscissa).

plotted as functions of γ in Fig. 13. There are two limiting tests for these results: (1) as c/h tends to zero, the results for $M/\mu h^2\alpha$ tend to the single inclusion result; (2) as c/h becomes large the results may be compared to the one obtained by Muskhelishvili for the rotation of a rigid stamp bonded to an elastic body (see [15], p. 492, eqn 114.19a). As may be seen in Fig. 13, the two limiting cases seem to support the accuracy of the calculated results.

The relationships established through an asymptotic expansion for the corner (c, h) were checked by calculating the values of the stress discontinuities at the corner, and substituting in eqns (3.16). The corner values were calculated by a quadratic extrapolation applied to the three points nearest that corner. It was found that eqns (3.16) were not satisfied; the size of the error was generally of the same order of magnitude as some of the individual terms. Even though an allowance must be made for the error introduced by the quadratic extrapolation, this size error is still considered large for the present type of analysis. To further consider this discrepancy, three of the relationships given in eqns (3.16) were incorporated in the system of $3N$ equations, by removing the equations closest to the corner (c, h) from the corresponding boundary conditions. This new system of equations yielded results which, away from the corner (c, h) matched the results previously obtained very closely (to four significant figures), and in addition, satisfied all of eqns (3.16). Moreover, the global results obtained using this new system of equations varied slightly from the ones obtained previously. To further test the sensitivity of the global results to the collocation scheme used, the order of the singularity at (c, h) was changed from $\zeta - 1 = -0.40484$ to -0.5, and the calculations were repeated with $N = 48$. Lastly, the singularities at (c, h) and $(c, 0)$ were set equal to -0.5, and a new set of results obtained for $N = 48$. A comparison of some of the results obtained from these solutions is given in Tables 3

Table 3. Vertical Displacement: Comparison of the portion of applied load carried by the sides of the block, calculated by: (1) Using the correct singularities ($\zeta - 1$, $\eta - 1$); (2) Using the correct singularities and three of the corner conditions; (3) Assuming square root singularity at (c, h); (4) Assuming square root singularity at both (c, h) and $(c, 0)$

Case \ c/h	Portion of applied load carried by the sides of block							
	0.05	0.1	0.2	0.3	0.5	1	2	4
1	0.7797	0.7079	0.6026	0.5349	0.4606	0.3658	0.2704	0.1927
2	0.7850	0.7109	0.6090	0.5444	0.4708	0.3741	0.2789	0.2027
3	0.7835	0.7106	0.6015	0.5315	0.4555	0.3592	0.2627	0.1837
4	0.7839	0.7098	0.5961	0.5242	0.4500	0.3503	0.2638	0.1832

Table 4. Vertical Displacement: Comparison of the error in the vertical displacement of the corner of the block $(c, 0)$ relative to $(0, 0)$ calculated by: (1) Using the correct singularities $(\zeta - 1;\ \eta - 1)$; (2) Using the correct singularities and three of the corner conditions; (3) Assuming square root singularity at (c, h); (4) Assuming square root singularity at both (c, h) and $(c, 0)$

Case	Vertical displacement of corner $(c, 0)$ relative to $(0, 0)$							
c/h	0.05	0.1	0.2	0.3	0.5	1	2	4
1	0.00191	0.00253	0.00197	0.00102	0.00115	0.00231	0.00255	0.00270
2	0.00191	0.00253	0.00197	0.00102	0.00115	0.00231	0.00255	0.00270
3	0.00192	0.00256	0.00203	0.00110	0.00124	0.00237	0.00257	0.00271
4	0.00059	0.00139	0.00051	−0.00061	−0.00017	0.00191	0.00252	0.00270

and 4. An examination of these tables shows that the global results remain relatively unaffected by small changes in the order of the corner singularities.

It should be noted that when the order of the singularities at both (c, h) and $(c, 0)$ was taken as -0.5, the related Jacobi polynomials reduced to the Chebyshev polynomials of the first kind (see, e.g. [13]). Numerical solutions of Cauchy-type singular integral equations with regular kernels obtained by use of the Gauss–Chebyshev integration formula, have been shown to converge to the correct results by Erdogan and Gupta[16], and Kalandiya[17]. Furthmore, Kalandiya states in[17] that this method was also successfully applied to problems with generalized kernels. Of course, as the singularities used here are not of the correct order, this method cannot be expected to yield correct results at the corners. However, the fact that the global results obtained by using the Gauss–Chebyshev integration formula match closely those obtained using the Gauss–Jacobi integration formula, as may be seen in Tables 3 and 4, tends to support the validity of the global results.

To investigate the rate of convergence of the global results, the number of points taken was varied at eight point intervals, from $N = 16$ to $N = 48$. Several of the calculated global results are presented in Tables 5 and 6. Table 5 shows the calculated values for the portion of the load carried by the sides of the block for the vertical displacement case. The variation of the ratio $M/\mu h^2\alpha$ with N, is shown for several values of c/h in Table 6. It is seen that the rate of convergence of these representative global quantities is quite satisfactory.

Although the accuracy of the global results obtained by use of the collocation scheme introduced in [10] has been shown to be satisfactory, the accuracy of the results in the vicinity of the corners is not certain. There are two reasons for this: (1) A second root is present at the corner (c, h) and is not taken into account; this root has a singular contribution of order

Table 5. Vertical Displacement: Variation of the amount of load carried by the sides of the block with the number of points used, for several values of c/h

N	Portion of applied load carried by the sides							
c/h	0.05	0.1	0.2	0.3	0.5	1	2	4
16	0.1684	0.6641	0.5622	0.4689	0.4010	0.3357	0.2380	0.1565
24	0.6411	0.7000	0.5815	0.5016	0.4313	0.3498	0.2529	0.1752
32	0.7458	0.7052	0.5916	0.5183	0.4460	0.3574	0.2612	0.1835
40	0.7721	0.7069	0.5981	0.5283	0.4548	0.3623	0.2666	0.1889
48	0.7797	0.7079	0.6026	0.5349	0.4606	0.3658	0.2704	0.1927

Table 6. Rotation: Variation of the ratio $M/\mu h^2\alpha$ with number of points used, calculated for several values of c/h

N	$M/\mu h^2\alpha$							
c/h	0.05	0.1	0.2	0.3	0.5	1	2	4
16	1.0457	1.1898	1.4789	1.8050	2.6216	5.6960	15.5036	49.1522
24	1.0541	1.1880	1.4750	1.8028	2.6226	5.6964	15.5096	49.2397
32	1.0557	1.1868	1.4731	1.8013	2.6213	5.6944	15.5088	49.2604
40	1.0558	1.1861	1.4720	1.8001	2.6196	5.6922	15.5070	49.2674
48	1.0558	1.1856	1.4712	1.7991	2.6179	5.6903	15.5054	49.2699

0.75904-1 = −0.24096 near that corner. As pointed out by Westmann in[8], although the stress field in the vicinity of the corner is dominated by the largest singularity, the presence of two singular terms may be important to the problem. (2) In two recent papers, [18, 19], Theocaris and Ioakimidis suggest that the collocation points as determined for the Gauss–Jacobi method may not be the correct ones. In [18], it is suggested that the rate of convergence of the results can be improved by a different choice of collocation points associated with the Gauss–Jacobi integration rule, or by using a different scheme such as the Lobatto rule. The collocation points for the case of real singularities are, respectively, the roots of the Jacobi-functions, and of their derivatives (see Elliot[20]). In [19], the problem of an antiplane shear crack terminating at a bimaterial interface solved by Erdogan and Cook[21], was reconsidered, and numerical results were obtained by using the modified Gauss–Jacobi and Lobatto–Jacobi methods discussed in [18]. It was found that while in general the results of [19] matched closely those of [21], the value of the stress intensity factor at the interface obtained by Theocaris and Ioakimidis was in much better agreement with the theoretical result than that obtained by Erdogan and Cook. However, the rate of convergence was not satisfactory. The authors attributed this to the existence of a second singularity of positive order near the interface. A technique is proposed for accounting for both singularities in the analysis, and this results in a much faster convergence of the results to the theoretical value. However, it should be realized that this technique could not be applied to the present analysis, since it deals with singularities of opposite signs.

In view of the arguments just presented, the accuracy of the corner values of the stress discontinuities obtained in the present analysis, by use of the collocation scheme introduced in [10], is uncertain.

Acknowledgements—The authors are grateful for support from the U.S. Air Force (G.K.H.) and from the National Science Foundation, Grant ENG 77-22155 (L.M.K.).

REFERENCES

1. R. Muki and E. Sternberg, On the diffusion of load from a transverse tension bar into a semi-infinite elastic sheet. *J. Appl. Mech.* **35**, 737 (1968).
2. E. Reissner, Note on the problem of the distribution of stress in a thin stiffened elastic sheet. *Proc. Nat. Acad. Sci.* **26**, 300 (1940).
3. R. Muki and E. Sternberg, On the diffusion of an axial load from an infinite cylindrical bar embedded in an elastic medium. *Int. J. Solids Structures* **5**, 587 (1969).
4. R. Muki and E. Sternberg, Elastostatic load-transfer to a half-space from a partially embedded axially loaded rod. *Int. J. Solids Structures* **6**, 69 (1970).
5. L. M. Keer and K. Chantaramungkorn, An elastic half plane weakened by a rectangular trench. *J. Appl. Mech.* **42**, 683 (1975).
6. I. N. Sneddon, *The Use of Integral Transforms*. McGraw-Hill, New York (1972).
7. A. Erdelyi (editor), *Tables of Integral Transforms* Vol. I. McGraw-Hill, New York (1954).
8. R. A. Westmann, Geometrical effects in adhesive joints. *Int. J. Engng Sci.* **13**, 369 (1975).
9. G. K. Haritos, *Stress Analysis of a Rigid Block Embedded in an Elastic Half Space*. Ph.D. Dissertation, Northwestern University (1978).
10. F. Erdogan, G. D. Gupta and T. S. Cook, Numerical solution of singular integral equations. *Methods of Analysis and Solutions to Crack Problems*, (Edited by G. C. Sih). Leyden Noordhoff, Amsterdam (1972).
11. M. L. Williams, Stress singularities resulting from various boundary conditions in angular corners of plates in extension. *J. Appl. Mech.* **19**, *TRANS. ASME*, **74**, 526 (1952).
12. A. H. Stroud and D. Secrest, *Gaussian Quadrature Formulas*. Prentice-Hall, Englewood Cliffs, New Jersey (1966).
13. M. Abramowitz and I. A. Stegun, *Handbook of Mathematical Functions*. Dover, New York (1965).
14. P. J. Davis, *Interpolation and Approximation*. Blaisdell, New York (1965).
15. N. I. Muskhelishvili, *Some Basic Problems of the Mathematical Theory of Elasticity*. Leyden Noordhoff, Amsterdam (1962).
16. F. Erdogan and G. D. Gupta, On the numerical solution of singular integral equations. *Quart. Appl. Math.* **30**, 525 (1972).
17. A. I. Kalandiya, *Mathematical Models of Two-Dimensional Elasticity*. Mir, Moscow (1975).
18. P. S. Theocaris and N. I. Ioakimidis, On the numerical evaluation of stress intensity factors. *Int. J. Fract.* **12**, 911 (1976).
19. P. S. Theocaris and N. I. Ioakimidis, Stress intensity factors and the tips of an antiplane shear crack terminating at a bimaterial interface, *Int. J. Fract.* **13**, 549 (1977).
20. D. Elliot, Uniform asymptotic expansions of the Jacobi polynomials and an associated function. *Math. Comp.* **25**, 309 (1971).
21. F. Erdogan and T. S. Cook, Antiplane shear crack terminating at and going through a bimaterial interface. *Int. J. Fract.* **10**, 227 (1974).

APPENDIX

The functions K_{Ni}, K_{Si}, L_{Ni} and L_{Si}, $i = 1, 2, \ldots, 7$, are given as

$$K_{N1}(x,y;s) = \frac{2(h-y)[(h-y)^2-(x-s)^2]}{[(h-y)^2+(x-s)^2]^2} + \frac{(\kappa^2-1)(h+y)}{(h+y)^2+(x-s)^2} + \frac{2\kappa(h-y)[(h+y)^2-(x-s)^2]}{[(h+y)^2+(x-s)^2]^2} - \frac{8hy(h+y)[(h+y)^2-3(x-s)^2]}{[(h+y)^2+(x-s)^2]^3} \tag{A1}$$

$$K_{S1}(x,y;s) = (x-s)\left\{\frac{2[(\kappa-2)(h-y)^2+\kappa(x-s)^2]}{[(h-y)^2+(x-s)^2]^2} + \frac{(\kappa^2+1)}{(h+y)^2+(x-s)^2} - \frac{4\kappa(h+y)^2}{[(h+y)^2+(x-s)^2]^2} + \frac{8hy[3(h+y)^2-(x-s)^2]}{[(h+y)^2+(x-s)^2]^3}\right\} \tag{A2}$$

$$K_{N2}(x,y;s) = (x-s)\left\{\frac{2[(\kappa+2)(h-y)^2+\kappa(x-s)^2]}{[(h-y)^2+(x-s)^2]^2} + \frac{(\kappa^2+1)}{(h+y)^2+(x-s)^2} + \frac{4\kappa(h+y)^2}{[(h+y)^2+(x-s)^2]^2} + \frac{8hy[3(h+y)^2-(x-s)^2]}{[(h+y)^2+(x-s)^2]^3}\right\} \tag{A3}$$

$$K_{S2}(x,y;s) = \frac{2(h-y)[(h-y)^2-(x-s)^2]}{[(h-y)^2+(x-s)^2]^2} - \frac{(\kappa^2-1)(h+y)}{(h+y)^2+(x-s)^2} + \frac{2\kappa(h-y)[(h+y)^2-(x-s)^2]}{[(h+y)^2+(x-s)^2]^2} + \frac{8hy(h+y)[(h+y)^2-3(x-s)^2]}{[(h+y)^2+(x-s)^2]^3} \tag{A4}$$

$$K_{N3}(x,y;s) = (x-s)\left\{\frac{2[(h-y)^2-(x-s)^2]}{[(h-y)^2+(x-s)^2]^2} - \frac{(\kappa^2+2\kappa-1)}{(h+y)^2+(x-s)^2} - \frac{4(h+y)[2h+\kappa(h-y)]}{[(h+y)^2+(x-s)^2]^2} + \frac{8hy[3(h+y)^2-(x-s)^2]}{[(h+y)^2+(x-s)^2]^3}\right\} \tag{A5}$$

$$K_{S3}(x,y;s) = \frac{2(h-y)[\kappa(h-y)^2+(\kappa+2)(x-s)^2]}{[(h-y)^2+(x-s)^2]^2} + \frac{(\kappa+1)^2(h+y)}{(h+y)^2+(x-s)^2} - \frac{2[2t-\kappa(y+t)][(y+t)^2-(x-s)^2]}{[(y+t)^2+(c-x)^2]^2} + \frac{8hy(h+y)[(h+y)^2-3(x-s)^2]}{[(h+y)^2+(x-s)^2]^3} \tag{A6}$$

$$K_{N4}(x,y;s) = -\frac{2(h-y)[\kappa(h-y)^2+(\kappa-2)(x-s)^2]}{[(h-y)^2+(x-s)^2]^2} + \frac{(\kappa-1)^2(h+y)}{(h+y)^2+(x-s)^2} - \frac{2[2h-\kappa(h+y)][(h+y)^2-(x-s)^2]}{[(h+y)^2+(x-s)^2]^2} + \frac{8hy(h+y)[(h+y)^2-3(x-s)^2]}{[(h+y)^2+(x-s)^2]^3} \tag{A7}$$

$$K_{S4}(x,y;s) = (x-s)\left\{\frac{2[(h-y)^2-(x-s)^2]}{[(h-y)^2+(x-s)^2]^2} + \frac{(\kappa^2-2\kappa-1)}{(h+y)^2+(x-s)^2} + \frac{4(h+y)[2h-\kappa(h-y)]}{[(h+y)^2+(x-s)^2]^2} - \frac{8hy[3(h+y)^2-(x-s)^2]}{[(h+y)^2+(x-s)^2]^3}\right\} \tag{A8}$$

$$K_{N5}(x,y;s) = \frac{(h-y)[(\kappa-1)(h-y)^2-(5-\kappa)(x-s)^2]}{[(h-y)^2+(x-s)^2]^2} + \frac{(3\kappa-1)(h+y)}{(h+y)^2+(x-s)^2} + \frac{2(3h-\kappa y)[(h+y)^2-(x-s)^2]}{[(h+y)^2+(x-s)^2]^2} - \frac{8hy(h+y)[(h+y)^2-3(x-s)^2]}{[(h+y)^2+(x-s)^2]^3} \tag{A9}$$

$$K_{S5}(x,y;s) = (x-s)\left\{\frac{[(\kappa-1)(h-y)^2+(3+\kappa)(x-s)^2]}{[(h-y)^2+(x-s)^2]^2} + \frac{(3\kappa+1)}{(h+y)^2+(x-s)^2} - \frac{4(h+y)(3h+\kappa y)}{[(h+y)^2+(x-s)^2]^2} + \frac{8hy[3(h+y)^2-(x-s)^2]}{[(h+y)^2+(x-s)^2]^3}\right\} \tag{A10}$$

$$K_{N6}(x,y;s) = -\frac{(h-y)[(3+\kappa)(h-y)^2+(\kappa-1)(x-s)^2]}{[(h-y)^2+(x-s)^2]^2} + \frac{(\kappa+1)(h+y)}{(h+y)^2+(x-s)^2} + \frac{2(h+\kappa y)[(h+y)^2-(x-s)^2]}{[(h+y)^2+(x-s)^2]^2} + \frac{8hy(h+y)[(h+y)^2-3(x-s)^2]}{[(h+y)^2+(x-s)^2]^3} \tag{A11}$$

$$K_{S6}(x,y;s) = (x-s)\left\{\frac{[5-\kappa)(h-y)^2-(\kappa-1)(x-s)^2]}{[(h-y)^2+(x-s)^2]^2} + \frac{(\kappa-1)}{(h+y)^2+(x-s)^2} - \frac{4(h+y)(h-\kappa y)}{[(h+y)^2+(x-s)^2]^2} - \frac{8hy[3(h+y)^2-(x-s)^2]}{[(h+y)^2+(x-s)^2]^3}\right\} \tag{A12}$$

$$K_{N7}(x,y;s) = (x-s)\left\{\frac{[(3+\kappa)(h-y)^2+(\kappa-1)(x-s)^2]}{[(h-y)^2+(x-s)^2]^2} - \frac{(\kappa-1)}{(h+y)^2+(x-s)^2} - \frac{4(h+y)(h-\kappa y)}{[(h+y)^2+(x-s)^2]^2} + \frac{8hy[3(h+y)^2-(x-s)^2]}{[(h+y)^2+(x-s)^2]^3}\right\} \tag{A13}$$

$$K_{S7}(x,y;s) = -\frac{(h-y)[(\kappa-1)(h-y)^2+(3+\kappa)(x-s)^2]}{[(h-y)^2+(x-s)^2]^2} + \frac{(\kappa+1)(h+y)}{(h+y)^2+(x-s)^2} - \frac{2(h+\kappa y)[(h+y)^2-(x-s)^2]}{[(h+y)^2+(x-s)^2]^2} + \frac{8hy(h+y)[(h+y)^2-3(x-s)^2]}{[(h+y)^2+(x-s)^2]^3} \tag{A14}$$

$$L_{N1}(x,y;t) = (c-x)\left\{-\frac{2[(\kappa-2)(y-t)^2+\kappa(c-x)^2]}{[(y-t)^2+(c-x)^2]^2} - \frac{(\kappa^2+1)}{(y+t)^2+(c-x)^2} + \frac{4\kappa(y+t)^2}{[(y+t)^2+(c-x)^2]^2} - \frac{8yt[3(y+t)^2-(c-x)^2]}{[(y+t)^2+(c-x)^2]^3}\right\} \tag{A15}$$

$$L_{S1}(x,y;t) = \frac{2(y-t)[(y-t)^2-(c-x)^2]}{[(y-t)^2+(c-x)^2]^2} + \frac{(\kappa^2-1)(y+t)}{(y+t)^2+(c-x)^2} - \frac{2\kappa(y-t)[(y+t)^2-(c-x)^2]}{[(y+t)^2+(c-x)^2]^2} - \frac{8yt(y+t)[(y+t)^2-3(c-x)^2]}{[(y+t)^2+(c-x)^2]^3} \tag{A16}$$

$$L_{N2}(x,y;t) = -\frac{2(y-t)[(y-t)^2-(c-x)^2]}{[(y-t)^2+(c-x)^2]^2} - \frac{(\kappa^2-1)(y+t)}{(y+t)^2+(c-x)^2} - \frac{2\kappa(y-t)[(y+t)^2-(c-x)^2]}{[(y+t)^2+(c-x)^2]^2} + \frac{8yt(y+t)[(y+t)^2-3(c-x)^2]}{[(y+t)^2+(c-x)^2]^3} \tag{A17}$$

$$L_{S2}(x,y;t) = (c-x)\left\{-\frac{2[(\kappa+2)(y-t)^2+\kappa(c-x)^2]}{[(y-t)^2+(c-x)^2]^2} - \frac{(\kappa^2+1)}{(y+t)^2+(c-x)^2} - \frac{4\kappa(y+t)^2}{[(y+t)^2+(c-x)^2]^2} - \frac{8yt[3(y+t)^2-(c-x)^2]}{[(y+t)^2+(c-x)^2]^3}\right\} \tag{A18}$$

$$L_{N3}(x,y;t) = \frac{2(y-t)[\kappa(y-t)^2+(\kappa+2)(c-x)^2]}{[(y-t)^2+(c-x)^2]^2} + \frac{(\kappa+1)^2(y+t)}{(y+t)^2+(c-x)^2} - \frac{2[2t+\kappa(y+t)][(y+t)^2-(c-x)^2]}{[(y+t)^2+(c-x)^2]^2} + \frac{8yt(y+t)[(y+t)^2-3(c-x)^2]}{[(y+t)^2+(c-x)^2]^3} \tag{A19}$$

$$L_{S3}(x,y;t) = (c-x)\left\{-\frac{2[(y-t)^2-(c-x)^2]}{[(y-t)^2+(c-x)^2]^2} + \frac{(\kappa^2+2\kappa-1)}{(y+t)^2+(c-x)^2} + \frac{4(y+t)[2t-\kappa(y-t)]}{[(y+t)^2+(c-x)^2]^2} - \frac{8yt[3(y+t)^2-(c-x)^2]}{[(y+t)^2+(c-x)^2]^3}\right\} \tag{A20}$$

$$L_{N4}(x,y;t) = (c-x)\left\{-\frac{2[(y-t)^2-(c-x)^2]}{[(y-t)^2+(c-x)^2]^2} - \frac{(\kappa^2-2\kappa-1)}{(y+t)^2+(c-x)^2} - \frac{4(y+t)[2t+\kappa(y-t)]}{[(y+t)^2+(c-x)^2]^2} + \frac{8yt[3(y+t)^2-(c-x)^2]}{[(y+t)^2+(c-x)^2]^3}\right\} \tag{A21}$$

$$L_{S4}(x,y;t) = \frac{2(y-t)[\kappa(y-t)^2+(\kappa-2)(c-x)^2]}{[(y-t)^2+(c-x)^2]^2} + \frac{(\kappa-1)^2(y+t)}{(y+t)^2+(c-x)^2} \frac{2[2x-\kappa(y+t)][(y+t)^2-(c-x)^2]}{[(y+t)^2+(c-x)^2]^2} + \frac{8yt(y+t)[(y+t)^2-3(c-x)^2]}{[(y+t)^2+(c-x)^2]^3} \tag{A22}$$

$$L_{N5}(x,y;t) = (c-x)\left\{-\frac{[(\kappa-1)(y-t)^2+(3+\kappa)(c-x)^2]}{[(y-t)^2+(c-x)^2]^2} - \frac{(3\kappa+1)}{(y+t)^2+(c-x)^2} + \frac{4(y+t)(3t+\kappa y)}{[(y+t)^2+(c-x)^2]^2} - \frac{8yt[3(y+t)^2-(c-x)^2]}{[(y+t)^2+(c-x)^2]^3}\right\} \tag{A23}$$

$$L_{S5}(x,y;t) = -\frac{(y-t)[(\kappa-1)(y-t)^2-(5-\kappa)(c-x)^2]}{[(y-t)^2+(c-x)^2]^2} + \frac{(3\kappa-1)(y+t)}{(y+t)^2(c-x)^2} + \frac{2(3t-\kappa y)[(y+t)^2-(c-x)^2]}{[(y+t)^2+(c-x)^2]^2} - \frac{8yt(y+t)(y+t)^2-3(c-x)^2]}{[(y+t)^2+(c-x)^2]^3} \tag{A24}$$

$$L_{N6}(x,y;t) = (c-x)\left\{-\frac{[(5-\kappa)(y-t)^2-(\kappa-1)(c-x)^2]}{[(y-t)^2+(c-x)^2]^2} - \frac{(\kappa-1)}{(y+t)^2+(c-x)^2} + \frac{4(y+t)(t-\kappa y)}{[(y+t)^2+(c-x)^2]^2} + \frac{8yt[3(y+t)^2-(c-x)^2]}{[(y+t)^2+(c-x)^2]^3}\right\} \tag{A25}$$

$$L_{S6}(x,y;t) = \frac{(y-t)[(3+\kappa)(y-t)^2+(\kappa-1)(c-x)^2]}{[(y-t)^2+(c-x)^2]^2} + \frac{(\kappa+1)(y+t)}{(y+t)^2+(c-x)^2} + \frac{2(t+\kappa y)[(y+t)^2-(c-x)^2]}{[(y+t)^2+(c-x)^2]^2} + \frac{8yt(y+t)[(y+t)^2-3(c-x)^2]}{[(y+t)^2+(c-x)^2]^3} \tag{A26}$$

$$L_{N7}(x,y;t) = \frac{(y-t)[(\kappa-1)(y-t)^2+(3+\kappa)(c-x)^2]}{[(y-t)^2+(c-x)^2]^2} + \frac{(\kappa+1)(y+t)}{(y+t)^2+(c-x)^2} - \frac{2(t+\kappa y)[(y+t)^2-(c-x)^2]}{[(y+t)^2+(c-x)^2]^2} + \frac{8yt(y+t)[(y+t)^2-3(c-x)^2]}{[(y+t)^2+(c-x)^2]^3} \tag{A27}$$

$$L_{S7}(x,y;t) = (c-x)\left\{-\frac{[(3+\kappa)(y-t)^2+(\kappa-1)(c-x)^2]}{[(y-t)^2+(c-x)^2]^2} + \frac{(\kappa-1)}{(y+t)^2+(c-x)^2} + \frac{4(y+t)(t-\kappa y)}{[(y+t)^2+(c-x)^2]^2} - \frac{8yt[3(y+t)^2-(c-x)^2]}{[(y+t)^2+(c-x)^2]^3}\right\}. \tag{A28}$$